Colloids and Surfaces B: Biointerfaces 239 (2024) 113933

Contents lists available at ScienceDirect

Colloids and Surfaces B: Biointerfaces

journal homepage: www.elsevier.com/locate/colsurfb

Deciphering the distinct biocontrol activities of lipopeptides fengycin and surfactin through their differential impact on lipid membranes

Guillaume Gilliard [a], Thomas Demortier [a], Farah Boubsi [b], M. Haissam Jijakli [c], Marc Ongena [b], Caroline De Clerck [d], Magali Deleu [a,*]

[a] Laboratory of Molecular Biophysics at Interfaces, UMRt BioEcoAgro 1158 INRAE, TERRA teaching and research centre, Gembloux Agro-Bio Tech, University of Liège, Gembloux 5030, Belgium
[b] Microbial Processes and Interactions laboratory, UMRt BioEcoAgro 1158 INRAE, TERRA teaching and research centre, Gembloux Agro-Bio Tech, University of Liège, Gembloux 5030, Belgium
[c] Integrated and Urban Plant Pathology Laboratory, UMRt BioEcoAgro 1158 INRAE, Gembloux Agro-Bio Tech, University of Liège, Gembloux 5030, Belgium
[d] AgricultureIsLife, UMRt BioEcoAgro 1158 INRAE, Gembloux Agro-Bio Tech, University of Liège, Gembloux 5030, Belgium

ARTICLE INFO

Keywords:
Lipopeptides
Membrane activity
Antifungal activity
Plant immunity

ABSTRACT

Lipopeptides produced by beneficial bacilli present promising alternatives to chemical pesticides for plant biocontrol purposes. Our research explores the distinct plant biocontrol activities of lipopeptides surfactin (SRF) and fengycin (FGC) by examining their interactions with lipid membranes. Our study shows that FGC exhibits a direct antagonistic activity against *Botrytis cinerea* and no marked immune-eliciting activity in *Arabidopsis thaliana* while SRF only demonstrates an ability to stimulate plant immunity. It also reveals that SRF and FGC exhibit diverse effects on membrane integrity and lipid packing. SRF primarily influences membrane physical state without significant membrane permeabilization, while FGC permeabilizes membranes without significantly affecting lipid packing. From our results, we can suggest that the direct antagonistic activity of lipopeptides is linked to their capacity to permeabilize lipid membrane while the stimulation of plant immunity is more likely the result of their ability to alter the mechanical properties of the membrane. Our work also explores how membrane lipid composition modulates the activities of SRF and FGC. Sterols negatively impact both lipopeptides' activities while sphingolipids mitigate the effects on membrane lipid packing but enhance membrane leakage. In conclusion, our findings emphasize the importance of considering both membrane lipid packing and leakage mechanisms in predicting the biological effects of lipopeptides. It also sheds light on the intricate interplay between the membrane composition and the effectiveness of the lipopeptides, providing insights for targeted biocontrol agent design.

1. Introduction

Biocontrol is a promising option to reduce the use of chemical pesticides that rises concerns regarding the impacts on human health and ecosystem degradation [1–4]. This approach consists in using natural mechanisms with the application of living organisms or derived molecules to reduce the effect of detrimental organisms and/or enhance growth of useful organisms such as crops [5]. Biocontrol agents can act either by direct antagonism against pests or by stimulating plant immunity to improve their responses against pathogen invasion [5]. The latter approach relies on a process called induced systemic resistance (ISR), where plant defense are potentiated by exogenous molecules, called elicitors, that can be synthetic or arising from living organisms such as microbes or plants [6–9].

In this context, cyclic lipopeptides (CLPs) produced by plant beneficial bacilli showed to be promising candidates as biocontrol agents as they present both direct antimicrobial activities and ability to stimulate plant defense [9–11]. Among the CLPs produced by *Bacillus*, the two most widely conserved families are surfactin (SRF) and fengycin (FGC) [12]. Each family presents specific structural traits (Fig. 1) that can influence their conformation, their interaction with membranes, but also their biological activities [13,14].

While FGC presents antifungal and antimicrobial activities, SRF is efficient against enveloped viruses [15,16] but does not show consistent

* Corresponding author.
E-mail address: magali.deleu@uliege.be (M. Deleu).

https://doi.org/10.1016/j.colsurfb.2024.113933
Received 29 February 2024; Received in revised form 24 April 2024; Accepted 26 April 2024
Available online 29 April 2024

antifungal activities [17–24] and requires much higher concentrations for antibacterial properties [13], with an effect mainly observed in synergy with other antimicrobial compounds [25]. The reported ability to stimulate plant immunity also varies between CLPs. In pathosystems involving dicotyledonous plants, ISR-activity of *Bacillus* CLPs showed to be driven by the presence of SRF and, to a lower extent, of FGC [17,26, 27]. In rice, a monocotyledonous plant, CLPs-mediated ISR showed a strong dependence to FGC with a minor contribution of SRF [18].

The biological activities of CLPs are supposed to originate from their ability to interact with lipids of the plasma membrane (PM) [9,14,28]. Due to their amphiphilic properties, CLPs readily insert into cell PM which can cause pore formation and membrane disruption contributing to their antimicrobial activities [14]. For this mechanism, the lipid composition of the targeted organism is important as it can affect the interaction of CLPs with PM and is supposed to drive the specificity of CLPs antimicrobial activities [14,23,29–32]. For plant immune stimulation, the mode of action is far to be understood but one hypothesis is that the insertion of CLPs would alter PM lipid organization triggering defense induction [9,10,33].

Lipids of PM present a huge molecular diversity that varies across kingdom and species and can be separated in three main classes: glycerolipids, sterols and sphingolipids [34–36]. These lipids also present a complex organization inside PM with an heterogenous lipid distribution between the two leaflets of PM (referred as membrane lipid asymmetry) but also lateral heterogeneities with the presence of membrane lipid domains, or raft, enriched in their sphingolipid and/or sterol content [35,37–39]. Accumulating evidence have shown the importance of this PM lipid segregation in biological processes [38–40]. However, the huge lipid molecular diversity of biological membranes makes complex the understanding of molecular determinants governing the role of PM lipids in cellular functions. Hence, artificial biomimetic membrane models, such as liposomes or lipid vesicles, supported lipid bilayers and lipid monolayers, have been developed as complementary tools allowing a fine-tune control on their lipid composition [34,40]. These models allow to disentangle more easily the relationship between a specific lipid molecule or lipid organization and the membrane activity of exogenous molecules. Nevertheless, as a simplified representation of biological systems, the relevance of membrane model studies has to be confirmed by biological studies [29,41].

In this study, we assessed how the effect of FGC and SRF on lipid membranes can be related to their biocontrol activities. In a first step, we compared their biocontrol activities by studying both their direct antagonism against the fungal pathogen *Botrytis cinerea* and their ability to stimulate *Arabidopsis thaliana* (hereafter *Arabidopsis*) immune response. In a second step, the membrane activity of the two CLPs was evaluated using liposomes as membrane models, with an easily tunable lipid composition, to detect the specificities in the interaction mechanism between CLPs and membrane lipids. Altogether, biological and biophysical results allowed us to delve into the significance of specific lipids or lipid properties in the eliciting and antifungal activities of CLPs.

2. Materials and methods

2.1. Lipopeptide purification

Surfactin (> 99% purity of a mix of homologues C12/C13/C14/C15 in relative proportions 7/17/45/31%) and fengycin (> 99% purity of a mix of isoform A and B in relative proportion 52/48%) were purified from spent supernatant of *B. velezensis* liquid culture as previously described [42–44].

Purity of the CLPs was checked by Ultra-Performance Liquid Chromatography (UPLC - Acquity H-class, Waters s.a., Zellik, Belgium) coupled to a single quadrupole mass spectrometer (Waters SQD mass analyzer) on an ACQUITY UPLC® BEH C_{18} 1.7 µm column. Elution was performed at 40°C with a constant flow rate of 0.6 mL/min using a gradient of acetonitrile and water both acidified with 0.1% formic acid as follows: 1 min at 30%, from 30% to 95% in 3.4 min and maintained at 95% for 2 min. Compounds were detected in electrospray positive ion mode by setting SQD parameters as follows: cone voltage 120 V, source temperature 130°C; desolvation temperature 400°C, and nitrogen flow: 1000 $L.h^{-1}$.

2.2. Plant growth conditions

Seeds of *Arabidopsis* Columbia ecotype Col-0 were disinfected for 2 min in ethanol 75%, 6 min in bleach 5° and rinsed three times in sterilized water. After the disinfection steps, seeds were grown on half strength Murashige and Skoog medium (M0222, Duchefa Biochimie) with addition of 1% (w/v) sucrose and 1.4% (w/v) agar, with a photoperiod of 12 h (100 µmol s^{-1} m^{-2}) and a temperature of 21°C.

For systemic immune activation assay, germinated seedlings were then transferred in Araponics systems containing nutritive solution (0.25% (v/v) FLORAMICRO®, 0.25% (v/v) FLORABLOOM®, 0.25% (v/v) FLORAGRO®; General Hydroponics®) and were grown during 3 weeks at 21°C under a photoperiod of 12 h (100 µmol s^{-1} m^{-2}).

2.3. Mycelial growth inhibition

B. cinerea isolate R16 [45] was taken out of the glycerol stock at −80°C and plated on Potato Dextrose Agar (PDA, Merck). The pathogen was then grown for 10 days in a chamber (23°C, 16D:8 N photoperiod) before use in the experiment. Round Petri dishes (Ø 90 mm) were filled with 35 mL of sterilized PDA containing 2.5, 10 or 20 µM of either SRF or FGC diluted in ethanol, or ethanol alone for the negative control. A 0.8 mm wide mycelial plug of *B. cinerea* grown for 10 days was placed in the center of each dish with the mycelium facing down. The dishes were sealed and placed for 5 days in the same growing chamber. The radius of each fungus was measured every 24 h. The Growth Inhibition factor (GI) was calculated at each time point as: $GI = \frac{Rc-R}{Rc}$ where Rc is the radius of the control and R is the radius of the treatment.

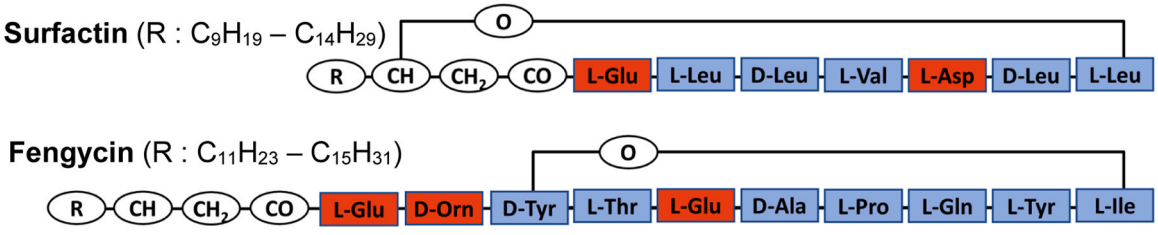

Fig. 1. Representative structure of surfactin and fengycin families. The canonical surfactin family displays a heptapeptide with two negative charges closed by a fatty acid chain (length ranging from C12 to C17) with a lactone bond. The fengycin family has a decapeptide with three charges (one positive and two negative) closed by an internal lactone ring and linked to a fatty acid chain with a length ranging from C14 to C18. Amino acid in red are charged residues and the ones in blue are neutral residues. [13].

2.4. Systemic immune activation assays

Four weeks-old plants grown in araponics were transferred in 50 mL falcons covered with aluminum foil and containing 45 mL of nutritive solution. SRF and FGC were then added in the falcons at a working concentration of 10 μM to perform treatment at the root level. The day after, leaf disks of 5 mm were cut form the fourth to the sixth leaves of the rosette and were transferred into a white 96-well microplate containing 150 μl of deionized water. The plate was incubated at room temperature in the dark overnight.

Measurement of apoplastic UPLC production was performed via a luminol-based chemiluminescence assay. Water was carefully removed and replaced by 90 μl of fresh deionized water before adding 10 μl of a 200 μM luminol L-012 + 10 μg/mL horseradish peroxydase solution. Luminescence signals were measured using a Spark Tecan multiplate reader. First, the background luminescence level was measured every minute during 5 min before adding 2 μl of a 5 mg/mL chitin suspension. After the addition chitin suspension, luminescence signals were measured every minute for 60 min (integration time = 1000 ms).

2.5. Root protoplast isolation

Roots from 12 to 15 days-old seedlings were cut into 1–2 mm segments and transferred to protoplasting solution (20 mM MES pH 5.7, 0.4 M mannitol, 20 mM KCl, 10 mM $CaCl_2$, 0.1% (w/v) BSA, 1.5% (w/v) cellulase R10, 0.4% (w/v) macerozyme R10) for 5 h at room temperature and in the dark. The suspension was then filtrated on gauze to eliminate root debris and the filtrate was centrifuged 6 min at 800 rcf. The supernatant was discarded and the pelleted protoplasts were rinsed once with W5 solution (4 mM MES pH 5.7, 154 mM NaCl, 125 mM $CaCl_2$, 5 mM KCl) before being resuspended in WI_{Ca} solution (2 mM MES pH 5.7, 0.5 M mannitol, 20 mM KCl, 2 mM $CaCl_2$) at a suitable concentration [46].

2.6. Calcium measurements with Fluo-4 AM on protoplasts

Protoplasts suspension (1–3 $_x10^5$ protoplasts / mL) isolated from roots of *Arabidopsis* col-0 was incubated for 1 h with 5 μM of fluo-4 AM (ThermoFischer) (from a 5 mM stock solution in DMSO). The suspension was then centrifuge at 700 rcf and the supernatant was discarded to eliminate the remaining free fluo-4 AM. The protoplasts were resuspended in fresh WI_{Ca} solution and were incubated for 1 h more. Then, wells of black 96-well microplates (Greiner Bio-One™ CellStar™, Fischer Scientific) were loaded with 100 μL of protoplasts solution per well. After the addition of 25 μL of 5 times concentrated treatment (i.e. a concentration of 50 or 100 μM of CLPs to reach a final concentration of 10 or 20 μM, respectively), the fluorescence was recorded every 15 sec using Spark® microplate reader (Tecan) with an excitation wavelength at 465 (±35) nm and an emission wavelength at 535 (±25) nm.

The values obtained were then converted as normalized fluorescence increase (F/F_0) by dividing the fluorescence measured at each time points (F) by the fluorescence measured at the first time point (F_0).

2.7. Composition of biomimetic liposomes

To mimic fungal PM, liposomes composed of 53 mol% 1-palmitoyl-2-oleoyl-glycero-3-phosphocholine (POPC), 22 mol% of 1-palmitoyl-2-oleoyl-sn-glycero-3-phospho-(10-rac-glycerol) (POPG) and 25 mol% of ergosterol were used. This model was based on the one developed by Monnier and co-workers to represent *B. cinerea* PM [47] with the presence of high amounts of ergosterol and a high ratio of anionic/zwitterionic phospholipids.

For liposomes mimicking plant PM, we used a lipid composition of 60 mol% 1-palmitoyl-2-linoleoyl-sn-glycero-3-phosphocholine (PLPC) to be representative of plant phospholipid acyl chains composed mainly of palmitic and linoleic acids [35,48], 20 mol% sitosterol (Sito) as it is the most abundant sterol in plants [35] and 20 mol% D-glucosyl-ß-1, 1′-N-palmitoyl-D-erythro-sphingosine (GluCer) as a commercially available plant sphingolipid [34] and an important lipid class for plant PM in terms of composition but also with a key role in its organisation [35,49].

2.8. Liposome preparation

1-palmitoyl-2-oleoyl-glycero-3-phosphocholine (POPC), 1-palmitoyl-2-oleoyl-sn-glycero-3-phospho-(10-rac-glycerol) (POPG), ergosterol, 1-palmitoyl-2-linoleoyl-sn-glycero-3-phosphocholine (PLPC), sitosterol (Sito) and D-glucosyl-ß-1,1′-N-palmitoyl-D-erythro-sphingosine (GluCer) were purchased from Avanti Polar Lipids and used without further purification. The different lipid mixtures of POPC-POPG (70:30 molar ratio), POPC-POPG-ergosterol (53:22:25 molar ratio), PLPC, PLPC-Sito (80:20 molar ratio) and PLPC-Sito-GluCer (60:20:20 molar ratio) were dispersed in a chloroform/methanol (Scharlau Lab Co.) (2/1; v/v) solution and dried under reduced pressure in a rotary evaporator and then kept under vacuum overnight. For laurdan and dynamic light scattering (DLS) analysis, the dried lipid films were then hydrated to 1 mM of lipids in MES 10 mM - NaCl 150 mM buffer at pH 5.8 during 1 h at 45°C with vortex mixing applied every 15 min and then subjected to five freeze/thaw cycles. For HPTS-DPX measurement, the lipid film was hydrated similarly but the lipid concentration was 3 mM and the hydration buffer also contained 30 mM of 8-hydroxypyrene-1,3,6 trisulfonic acid (HPTS) and 50 mM of p-xylene-bis-pyridinium bromide (DPX). The dispersions were finally extruded fifteen times through two stacked Nuclepore 100 nm polycarbonate filters using a Lipex Biomembranes (Vancouver, BC) extruder to obtain LUVs.

2.9. HPTS-DPX leakage assays

Membrane leakage assays were based on measurements of the release of a fluorescent dye (in this case HPTS) previously co-encapsulated inside liposomes with a quencher (in this case, DPX). Upon leakage, the dye and its quencher become highly diluted in extravesicular media which dissociates the dye and the quencher leading to an increase in fluorescence [50].

Following extrusion, liposome suspension was flowed through a Sephadex-G75 (Cytiva) gel purification column to remove the unencapsulated dye. The Sephadex gel was obtained by hydrating 1 g of Sephadex G75 with 30 mL of distilled water at 150 °C for 2 h under shaking at 200 rpm with a magnetic stirrer. The Sephadex gel was conditioned with 20 mL of MES 10 mM - NaCl 150 mM buffer at pH 5.8 before liposome purification.

After purification, liposome suspension was diluted to a concentration of 100–200 μM of lipid and this solution was loaded in wells of a black 96-well microplate (Greiner Bio-One™ CellStar™, Fischer Scientific) with a volume of 100 μL per well. The fluorescence was recorded once before treatment and every 2 min until 44 min after the addition of 25 μL of 5 times concentrated treatments (i.e. 12.5, 25, 50, 75, 100, 125 and 250 μM of CLPs to reach 2.5, 5, 10, 15, 20, 25 and 50 μM of final concentration, respectively) using Spark® microplate reader (Tecan) with an excitation wavelength at 465(±35) nm and an emission wavelength at 535(±25) nm.

Percentage of membrane leakage was defined as $(F_t\text{-}F_0)/(F_{max}\text{-}F_0)_X100$, where F_t is the fluorescence measured at each time point, F_0 is the fluorescence measured before the addition of treatments and F_{max} is the maximum fluorescence signal obtained after complete membrane disruption with 0.2% of Triton X-100.

2.10. Laurdan polarization on root protoplasts and lipid vesicles

Protoplast suspension (1–3 $_x10^5$ protoplasts / mL) or 100 μM lipid vesicle preparation (from a stock solution at 1 mM) was incubated with 1 μM of laurdan (Sigma-Aldrich) for 1h30. Then, wells of a black 96-well

microplate (Greiner Bio-One™ CellStar™, Fischer Scientific) were loaded with 100 µL of protoplasts or lipid vesicle solution per well.

The fluorescence was then recorded twice before treatment and every 2 min until 44 min (for liposomes) or every 2.5 min for 20 min (for protoplasts) following the addition of 25 µL of 5 times concentrated treatment (i.e. 12.5, 25, 50, 100 and 250 µM of CLPs to reach 2.5, 5, 10, 20 and 50 µM of final concentration, respectively) using Spark® microplate reader (Tecan) with an excitation wavelength at 360(±35) nm and emission wavelengths at 430(±20) nm and 485(±20) nm.

The generalized polarization (GP) was defined as $GP = \frac{(I_{430nm} - I_{485nm})}{(I_{430nm} + I_{485nm})}$, were $I_{430\,nm}$ and $I_{485\,nm}$ represents the blank-subtracted fluorescence intensities at emission wavelengths of 430 nm and 485 nm respectively. Variation of GP (ΔGP) is defined as the subtraction of GP measured at each time point following treatment and GP measured before treatment.

Blank measurements were carried out on samples containing the different concentrations of CLPs but which were not stained with laurdan. In all blanks tested, no specific fluorescence signal was observed for FGC or SRF.

2.11. Dynamic light scattering measurements on liposomes

Dynamic light scattering (DLS) measurements were performed on liposome solution at different concentrations of SRF or FGC (0, 10, 20, 40, 75 and 187.5 µM). One mL of vesicle solution (lipid concentration of 300 µM) was placed in a cuvette for DLS measurement. The scattered intensity was measured at 25.0 °C using a Zetasizer Nano DLS instrument (Malvern Panalytical) to obtain the liposome size and the derived count rate, in kilo counts per second (kcps). After a first measurements to get liposome size and derived count rate without CLPs, SRF or FGC from a stock solution of 0.5 mM were added successively in the liposome solution to obtain the evolution of liposome size with increasing CLP concentration. Measurements were performed three times on each sample to ensure reproducibility (eight acquisitions per measurement with an acquisition time of 10–15 sec).

3. Results

3.1. Antifungal property and stimulation of plant cell immune responses

The direct antagonistic activity of SRF and FGC was evaluated against *B.cinerea,* a fungal pathogen of high scientific and economic importance responsible for both pre- and post-harvest crop losses [51]. The effect of SRF and FGC was evaluated by comparing the growth of the pathogen on PDA amended with several CLPs concentrations to its growth on PDA without CLPs (Fig. 2a, b). In presence of FGC, we observed a significant reduction of *B. cinerea* growth in the same order of magnitude for all the concentrations used, with an inhibition of growth (GI) after 72 h of about 50% in presence of FGC. The fungal growth in presence of SRF did not show any difference with growth in absence of CLPs. Hence, in accordance with previous studies [17–24], biocontrol activity of SRF does not rely on a direct antagonism while FGC can inhibit the fungal growth through a direct toxicity against fungi.

In our experimental conditions, the effect of FGC on fungal growth did not show a typical dose-response effect, in accordance with the work by Wise and coworkers [23] on different fungal strains including *B. cinerea*. Nevertheless, our range of concentrations tested, all higher than the critical micellar concentration of fengycin [52], remains limited compared to other studies [21,22] which may explain the absence of a visible dose-response effect.

The stimulation of plant immunity by CLPs was evaluated by analyzing the systemic activation of immune response of *Arabidopsis* pre-treated with CLPs and by analyzing the variation of cytosolic calcium ($[Ca^{2+}_{cyto}]$) in protoplasts from *Arabidopsis* roots.

To assess the systemic immune activation (SIA), we studied the potentiation of immune responses in leaves of plant pre-treated with CLPs at the root level. After pre-treatments, we measured the production of apoplastic reactive oxygen species (ROS_{apo}) in leaf disks of plant in response to a stimulation with chitin, a well-known plant elicitor [53]. The SIA assays revealed that *Arabidopsis* plants pre-treated at the root level with 10 µM SRF, a concentration previously determined as the minimal active concentration [17,54], show an increased ROS_{apo} production in response to chitin treatment compared with non-pretreated plants (Fig. 3a, c). In contrast, plants pre-treated with 10 µM FGC show a similar ROS_{apo} production in response to chitin than plants

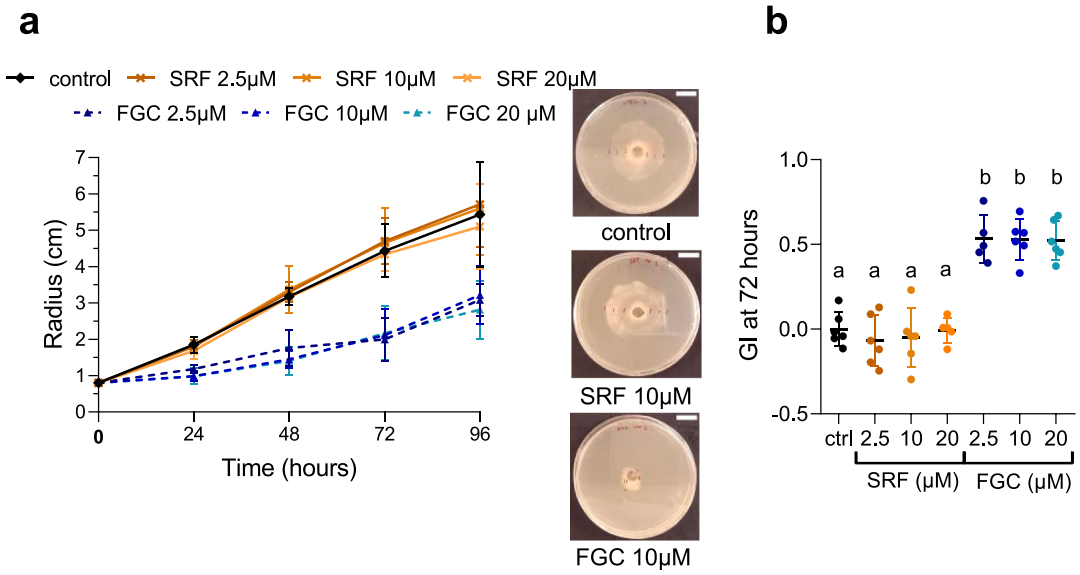

Fig. 2. Impact of surfactin (SRF) and fengycin (FGC) on the mycelial growth of *B. cinerea* (a) Time-course evolution of *B. cinerea* mycelial growth on PDA in presence of 0.1% ethanol (control), 2.5 µM, 10 µM and 20 µM SRF and 2.5 µM, 10 µM and 20 µM FGC. Images show representative pictures of *B. cinerea* mycelial growth after 72 h in presence of 0.1% ethanol (negative control), 10 µM SRF and 10 µM FGC. Scale bar in upper right represents 15 mm. (b) Growth inhibition factor (GI) of *B. cinerea growth* with surfactin and fengycin treatments after 72 h. Letters indicate statistically different groups at α = 0.05 (one-way ANOVA and Tukey's multiple-comparison post-test). Data in (a) and (b) represents mean ± SD (n=6) from two independent experiments.

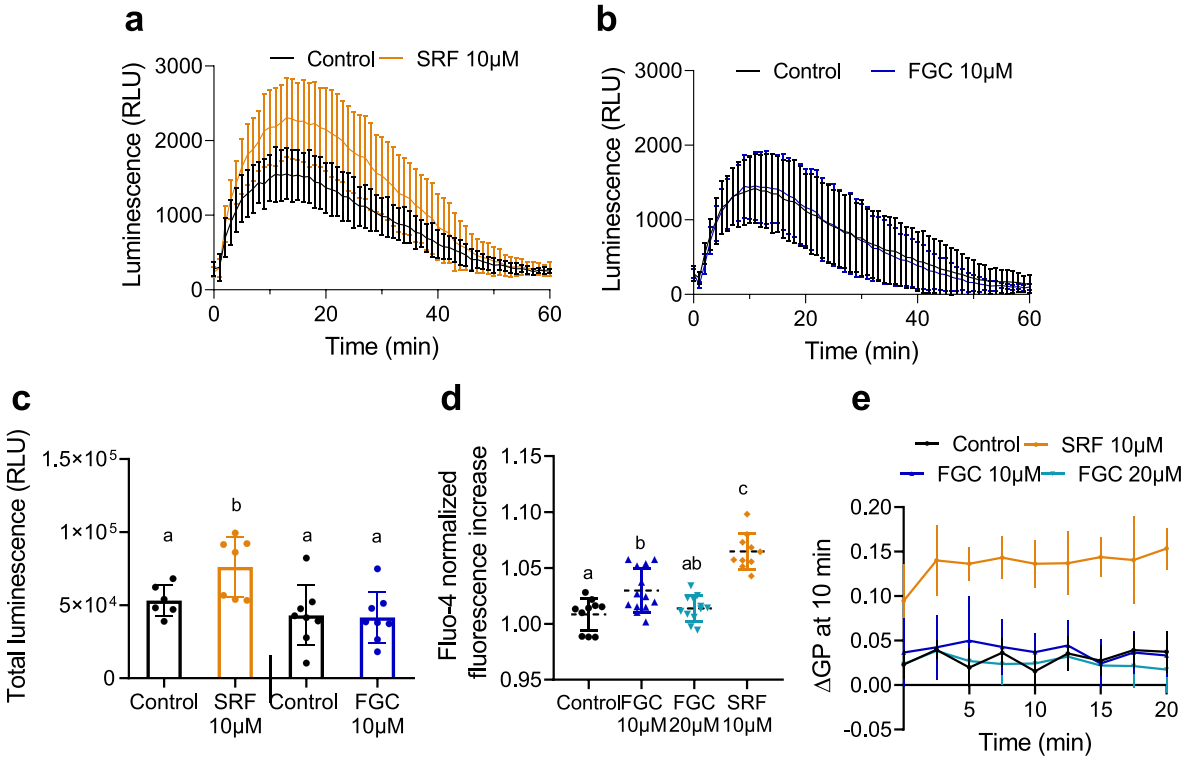

Fig. 3. Effect of fengycin (FGC) and surfactin (SRF) on plant cell immune stimulation and plasma membrane mechanics (a-b) Kinetics of ROS_{apo} production measured with luminescence assay following treatment with 250 µg/mL chitin in leaf disk of *Arabidopsis* pre-treated at the root level with 10 µM SRF (a) or 10 µM FGC (b) compared to control pre-treatment (0.1% ethanol). Results show the mean luminescence ± SD (n≥6). (c) Total ROS_{apo} production measured with luminescence assay following treatment with 250 µg/mL chitin in leaf disk of *Arabidopsis* pre-treated at the root level with 10 µM SRF, 10 µM FGC or control pre-treated (0.1% ethanol). Results show the mean total luminescence ± SD (n≥6), obtained by the sum of all detected luminescence values. Letters represent statistically different groups at α = 0.05 (one-way ANOVA and Neuwman-Keuls multiple comparison post-tests). (d) $[Ca^{2+}_{cyto}]$ elevation detected with Fluo-4 in root protoplasts of *Arabidopsis* Col-0 after control treatment or treatment with 10 µM SRF, 10 µM FGC or 20 µM FGC. Data shows mean ± SD (n≥10) of normalized fluorescence increase of Fluo-4 five minutes after treatments. Letters represent statistically different groups at α = 0.05 (one-way ANOVA and Tukey's multiple-comparison post-test). (e) Change of laurdan generalized polarization (ΔGP) measured in *Arabidopsis* root protoplasts after control treatment or treatment with 10 µM SRF, 10 µM FGC or 20 µM FGC. Data are represented as mean GP variation ± SD (n=6) compared to GP measured before the addition of treatment.

pre-treated with control solution (Fig. 3b, c).

To complete the analysis of CLP's effect on plant immunity, measurements of $[Ca^{2+}_{cyto}]$ variation in root protoplasts were performed. Treatment with 10 µM SRF induced a significant $[Ca^{2+}_{cyto}]$ increase while FGC treatment showed significantly lower $[Ca^{2+}_{cyto}]$ responses, even at concentration twice higher than for SRF (Fig. 3**d,** Suppl Fig1 for time course measurements).

Since the ability of CLPs to stimulate plant immune responses is believed to originate from their interaction with plant PM, we used the facilitated access to PM allowed by protoplasts to investigate the possible effect of CLPs on PM mechanics. Using the solvatochromic probe laurdan, sensitive to membrane hydration and thus to lipid packing [55], we analyzed the variation of PM fluidity in root protoplasts with the two CLPs. No effect on PM lipid packing was observed for FGC contrary to SRF that increased lipid compaction (Fig. 3e).

The correlation between the effect of CLPs on fluidity of protoplast PM and their ability to induce a $[Ca^{2+}_{cyto}]$ responses and SIA agrees with the hypothesis of plant immune stimulation by CLPs based on their ability to interact with plant PM [33] and suggests that FGC is very poorly susceptible to stimulate immunity in *Arabidopsis* contrary to SRF.

3.2. Membrane activity on liposomes mimicking fungal and plant plasma membranes

The biological activities of CLPs likely rely on their ability to insert into membranes and alter lipid membrane properties [14,29,33]. As SRF and FGC exhibit distinct plant biocontrol activities, we investigated whether distinct characteristics in the membrane activity of CLPs could account for these differences. For this purpose, we used liposomes mimicking fungal or plant PM to assess the effect of CLPs on membrane permeabilization and fluidity. The permeabilization, or leakage, assays were conducted by measuring the efflux of HPTS-DPX initially encapsulated within the liposomes. It indicates the ability of CLPs to disrupt and possibly form pores into membranes. This property has been correlated with induction of cell leakage and cell death leading to antimicrobial properties [29,30,32,41,56]. Membrane fluidity experiments on liposomes were performed with the laurdan probe as on protoplasts. Since analysis of membrane activity with liposomes can depend on the lipid concentration [32,57], we analysed our data using the CLPs-to-lipid molar ratio (ratio between CLPs and lipid concentrations, in molar) rather than CLPs concentration only.

Distinct behaviour between the two CLPs was observed in leakage and fluidity assays (Fig. 4). For both models, FGC induced membrane leakage at much lower CLPs-to-lipid ratio than SRF. A leakage was already observed at a ratio of 0.06 for FGC while leakage started progressively at ratios higher than 0.12 for SRF (Fig. 4a, e). The shape of dye efflux was also different for each CLP on both lipid models. The leakage induced by FGC shows a steep increase at low ratio that stabilizes to a plateau while the leakage induced by SRF increased more progressively with increasing CLPs-to-lipid ratio. In contrast to leakage and in accordance with assays on protoplasts, membrane fluidity was more affected by SRF with a slight effect observable at a ratio of 0.12 that progressively increased while FGC effect on membrane fluidity remained low even at high CLPs-to-lipid ratio (Fig. 4b, f).

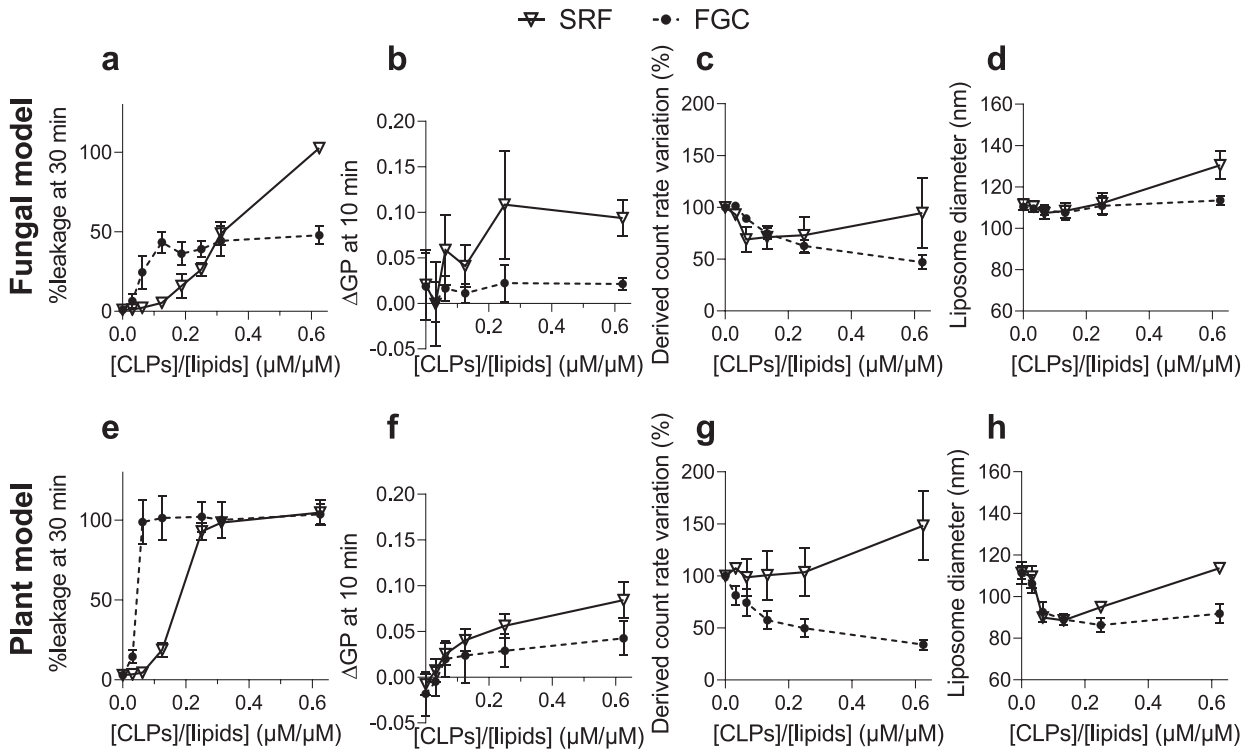

Fig. 4. Effect of fengycin (FGC) and surfactin (SRF) on liposomes mimicking fungal (a to d) and plant (e to h) plasma membranes as a function of the CLPs-to-lipid molar ratio. (a, e) Membrane leakage measured with HPTS-DPX in lipid vesicles (final lipid concentration of 80 μM) composed of POPC-POPG-ergosterol (53:22:25 molar %) as fungal model (a) and PLPC-sito-GluCer (60:20:20 molar %) as plant model (e) 30 min after the addition of increasing concentration of FGC or SRF. Data are represented as % of leakage ± SD (n=6 for 0 μM, n=4 for the other concentrations) compared to leakage observed with the addition of 0.2% Triton X-100. (b, f) Change of laurdan generalized polarization (GP) in lipid vesicles (final lipid concentration of 80 μM) composed of the fungal model (b) and the plant model (f) 10 min after the addition of increasing concentration of FGC or SRF. Data are represented as mean GP variation ± SD compared to GP measured before the addition of treatment. (n=4 for fungal model, n=10 for plant model – SRF, n=8 for plant model - FGC). (c, d, g, h) Liposomes diameter (c, g) and variation of derived count rates (d, h) (mean ± SD, n=6) measured with dynamic light scattering with increasing concentration of FGC or SRF. The initial lipid concentration was 300 μM. All measurements in the figures come from data obtained from at least 2 independent batches of liposomes.

Results from membrane models suggest that FGC effects are more related to its ability to disrupt and/or permeabilize lipid membranes while SRF insertion leads to changes in membrane structure and/or organization rather than membrane permeabilization, especially at low CLPs-to-lipids ratios. To confirm the permeabilizing effect observed for FGC but not SRF, we measured the liposome diameter and the derived count rate by dynamic light scattering (DLS). The derived count rate measures the strength of light scattering signal of the sample and is thus influenced by both the number and the size of liposomes in the medium [58,59] (a higher derived count rate indicates higher number of particles, larger particles, or higher number and larger particles in the medium). In the presence of a permeabilizing effect, a reduction of liposome number and/or size can be expected. In the fungal model, the presence of FGC has low impact on liposome size while SRF shows a slight increase in liposome diameter at high CLPs-to-lipid ratio (Fig. 4d). In the plant model, a slight reduction of liposome size was observed at low CLPs-to-lipid ratio for both CLPs. At higher CLPs-to-lipid ratio, an increase of liposome size was observed for SRF while the liposome size remains stable for FGC (Fig. 4h). In addition to size measurements, a progressive reduction of the derived count rate was noticed with increasing FGC concentrations in both models (Fig. 4 c, g). In the fungal model, the stable liposome size with a decreasing count rate in presence of FGC indicates a reduction in the number of liposomes. This agrees with the hypothesis that FGC acts by permeabilizing liposomes. In the plant model, the effect of FGC at low ratios on the derived count rate can originate from both its impact on liposome size and a permeabilizing effect, explaining a steeper decrease in the plant model compared to the fungal model, while at higher ratios, the decrease in the derived count rate with no change in liposome size also support a permeabilizing mechanism. In contrast, the presence of SRF has only a small effect on the derived count rate in the fungal model and slightly increased the derived count rate at high CLPs-to-lipid ratio in the plant model (Fig. 4c, g). This increase coincides with an observed increase in liposome size at high SRF-to-lipid ratio. Hence, it is likely that the increase in derived count rate by SRF comes from its impact on liposome size rather than an impact on the liposome number. The absence of effect of SRF on liposome number supports the idea that SRF does not act through a permeabilizing mechanism but modifies the global structure of the liposome bilayer which could lead to liposome fusion at high SRF-to-lipid ratio.

3.3. *Lipid specificity of the interaction with biomimetic liposomes*

The lipid composition is a key parameter for CLPs biological activities. In particular, ergosterol was found to be a crucial determinant for the selectivity of the fungicidal activity of CLPs [23,29,60] and sphingolipids of plant PM was suggested as a preferential interactant for SRF [9]. We therefore investigated the lipid specificity of CLPs membrane disturbance through the modulation of liposome lipid composition (Fig. 5). For the fungal model, we evaluated the importance of ergosterol by comparing CLPs membrane activity obtained with the model POPC-POPG-ergosterol (53:22:25 molar ratio) with a second model POPC-POPG (70–30 molar ratio) that keeps the same anionic/zwitterionic lipid ratio but does not contain ergosterol. For plant model, we focused on the importance of sphingolipids and sterols and compared CLPs membrane activity on liposomes with the entire lipid composition

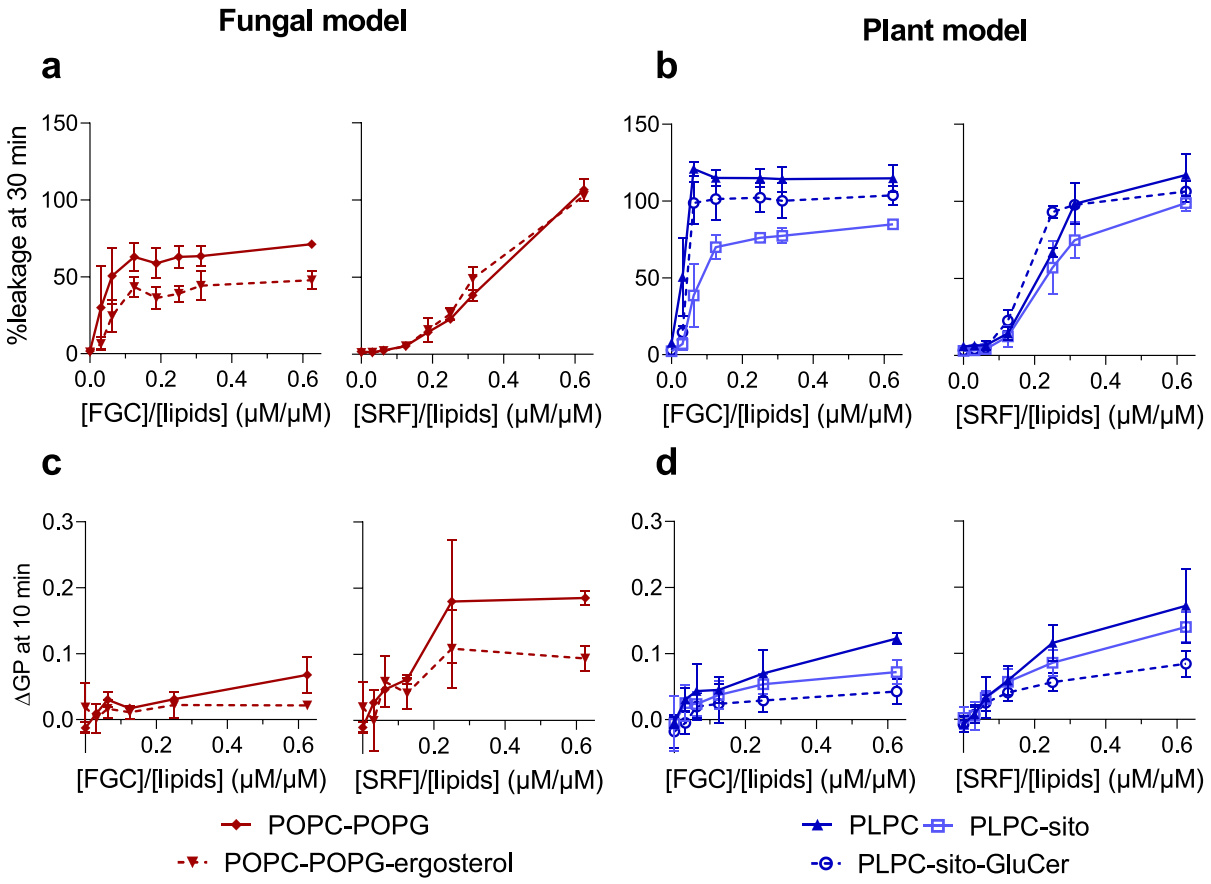

Fig. 5. Lipid specificity of membrane activity of fengycin (FGC) and surfactin (SRF) on fungal (a, c) and plant biomimetic liposomes (b, d) as a function of the CLPs-to-lipid molar ratio. (a, b) Membrane leakage measured with HPTS-DPX in lipid vesicles (final lipid concentration of 80 μM) composed of POPC-POPG (70:30 molar %) and POPC-POPG-ergosterol (53:22:25 molar %) in (a) and PLPC, PLPC-sito (60:20 molar %) and PLPC-sito-GluCer (60:20:20 molar %) in (b) 30 min after the addition of increasing concentration of FGC (left) or SRF (right). Data are represented as % of leakage ± SD (n=6 for 0 μM, n=4 for the other concentrations) compared to leakage observed with the addition of 0.2% Triton X-100. (c, d) Change of laurdan generalized polarization (GP) in lipid vesicles (final lipid concentration of 80 μM) composed of POPC-POPG (70:30 molar %) and POPC-POPG-ergosterol (53:22:25 molar %) in (c) and PLPC, PLPC-sito (60:20 molar %) and PLPC-sito-GluCer (60:20:20 molar %) in (d) 10 min after the addition of increasing concentration of FGC (left) or SRF (right). Data are represented as mean GP variation ± SD (n≥4) compared to GP measured before the addition of treatment. All measurements in the figures comes from data obtained from 2 independent batches of liposomes.

PLPC-sito-GluCer (60:20:20 molar %), liposomes containing PLPC-sito (80:20 molar %) without sphingolipids and liposomes containing only PLPC.

In all the lipid compositions tested, FGC-induced leakage showed a similar shape with a steep increase in dye efflux at low ratio (between 0.03 and 0.12) that stabilizes around a plateau for ratios higher than 0.12. The presence of a sterol, either ergosterol or sitosterol, reduced the leakage effect of FGC that occurred at higher CLPs-to-lipid ratio than without sterols (0.06 for POPC-POPG-ergosterol and PLPC-sito vs 0.03 for POPC-POPG and PLPC, respectively) and with a lower magnitude (maximum dye efflux of around 40% for POPC-POPG-ergosterol and 75% for PLPC-sito vs 65% for POPC-POPG and 100% for PLPC) (Fig. 5a, b). Interestingly, the presence of both sterols and sphingolipids in the plant model suppressed the inhibitory effect of sterols as a similar leakage was observed for liposomes composed of PLPC and PLPC-sito-GluCer. Comparison of FGC-induced leakage between fungal and plant models also revealed a much lower leakage in fungal models compared to plant models.

For SRF, leakage was more progressive and occurred at higher CLPs-to-lipid ratio than FGC (Fig. 5a, b). SRF-induced leakage was also less impacted by the presence of sterols, even though, for plant models, a slight reduction of dye efflux can be noticed for PLPC-sito compared to PLPC. Intriguingly, the presence of sphingolipids increases SRF-induced leakage with a complete leakage reached at a CLPs-to-lipid ratio of 0.25 for PLPC-sito-GluCer liposomes, 0.31 for PLPC and 0.63 for PLPC-sito. Comparison of SRF-induced leakage between fungal and plant models also revealed a slightly lower leakage in the fungal model but the difference was less pronounced than the one observed for FGC.

Regarding membrane fluidity, we observed a gradual reduction of FGC and SRF effect with increasing lipid complexity but for all lipid composition, SRF had a higher impact on membrane fluidity than FGC (Fig. 5c, d). When looking at the initial lipid packing of the different compositions without CLPs, measured with laurdan generalized polarisation (GP), we observed that models with the highest initial lipid packing (i.e. PLPC-sito-GluCer with an initial GP of −0.11±0.04 and POPC-POPG-ergosterol with an initial GP of −0.16±0.04) are the less sensitive to CLPs-induced rigidification (Fig. 5c, d, Suppl Fig. 2). At the opposite, the model with only PLPC or POPC-POPG, whose fluidity was the most affected by CLPs, are the most fluid model between the ones tested (with a GP of −0.35±0.06 for PLPC and −0.31±0.03 for POPC-POPG). Hence, a model presenting already a high lipid packing is less prone to undergo further compaction of their lipids.

4. Discussion

4.1. Disturbance of membrane lipid packing as an additional mechanism to membrane leakage for CLPs biological activities

SRF and FGC showed to affect lipid membrane through distinct processes. While SRF strongly affects membrane physical state but was less prone to induce membrane permeabilization, FGC showed the opposite with a strong ability to permeabilize membrane without marked effect on its lipid packing.

Differences in membrane activity between SRF and FGC have already been discussed in their leakage mechanism on liposomes, with a graded leakage effect observed for SRF while FGC showed an all-or-none leakage mechanism [29,32,61,62]. A graded leakage is characterized by a progressive and transient release of the dye from all vesicles while the all-or-none leakage shows a more heterogenous dye efflux with a fraction of vesicles releasing all their dyes while the other fraction keeps the dye entirely entrapped. The graded process originates from a phenomenon that dissipates upon leakage such as an asymmetric insertion of molecules in the outer leaflet. This asymmetric insertion causes differential stress between the two leaflets due to imbalance in area density of molecule between leaflets [63]. It leads to transient mechanical failure of the membrane to release the stress, followed by the annealing of membrane [64]. The presence of differential stress into membrane has recently been shown to impact important membrane properties such as tension [65] and could therefore explain the observed impact of SRF on membrane fluidity, which has also been reported previously for DOPC:DPPC vesicles [66]. The all-or-none process arises from the stabilization of defects or pore-like structures in the membrane by covering their edges with a rim enriched in membrane-active molecules [41,64]. This process seems to impact less the membrane lipid packing as we observed lower impact of FGC on membrane fluidity compared to SRF. Such low impact on membrane fluidity of FGC has also been observed on DPPC membranes, where FGC showed to mainly affect the polar headgroup regions but not the hydrophobic core [67]. Nevertheless, the low impact on membrane fluidity does not exclude an impact on the global distribution of membrane domains as it was observed in DOPC:DPPC bilayer [68]. Hence, the effect of CLPs on both membrane leakage and membrane lipid packing could represent two complementary indicators of their specific mechanism of membrane destabilization.

The differences in interaction mechanisms of SRF and FGC with lipid membranes has been suggested as an explanation for their specificities in antimicrobial activities [29,32]. The all-or-none leakage mechanism has indeed shown good correlation with antimicrobial properties which is not the case for the graded leakage. Hence the difference in antifungal activities between SRF and FGC, noted in our study and previous ones [18,21,22,69], can be related to an efficient membrane disruption and/or permeabilization for FGC (in accordance with its all-or-none leakage mechanism). In contrast, the effect of SRF on membrane lipid packing and its graded leakage effect may be less effective to disrupt biological membranes. This distinction could also account for antibacterial activities where SRF may require high dose or synergic compounds to be effective [13,25].

However, altering PM physical properties may be responsible for other important biological activities. PM is a flexible and dynamic structure capable of sensing and transducing mechanical signals inside the cell due to its highly dynamic physical properties [70,71]. PM organization has been shown to be crucial for immune responses in plants [72]. Modifying PM physical properties can activate PM signalling proteins [73,74]. This could explain the very low effect of FGC on plant responses as FGC does not alter membrane physical properties. In contrast SRF, able to increase the PM lipid packing, triggers a marked $[Ca^{2+}_{cyto}]$ influx in protoplasts and potentiates ROS_{apo} responses in leaves while applied at the root level. Hence, our observations suggest that the distinct effect of SRF and FGC on plant PM properties contributes to their difference in plant eliciting activity.

4.2. Modulation of CLPs' membrane activity by membrane lipid composition

CLPs' activities on both fungal and plant plasma membrane models were negatively impacted by the presence of sterols. Interestingly, the combination sterols-sphingolipids in plant models tended to reduce the impact on membrane lipid packing but it also compensated the sterol effects on leakage and even improved leakage for SRF. Sterols and sphingolipids are known to be key players for membrane organization and lipid packing since changes in their proportion modulate the presence of lipid domains in membrane [35,38,75].

The influence of sterols could come from their ability to increase membrane packing [75]. Previous studies have observed that a higher lipid packing can impede the insertion of SRF [28,66,76] and FGC [44], resulting in a lower membrane disturbance. Sterols were also found to reduce the depth of insertion of other CLPs from the viscosin groups produced by *Pseudomonas* spp. [77]. FGC presents a longer acyl chain than SRF and also possesses two amino acids outside the peptide ring, while SRF has all its amino acids inside the peptide ring (Fig. 1). This may suggest that acyl chain of FGC will insert more deeply inside the membrane than the acyl chain of SRF. Since sterols are located in the hydrophobic core of the lipid bilayer and hinder a deep insertion of CLPs, they are likely to further affect molecules that insert deeper into the membrane. This could explain why sterols impact FGC-induced leakage but have minimal impact on SRF-induced leakage, as previously observed [29,78]. In the case of FGC, the effect of sterols correlates with its lower antifungal effects on plant pathogen with higher ergosterol content [23].

Regarding the addition of sphingolipids to the sterol-containing model, interaction between sphingolipids and sterols are known to modulate the lateral lipid distribution with the formation of raft domains with more tightly packed lipids [79–81]. The presence of sphingolipids could therefore increase the lateral heterogeneity of the membrane, creating some packing defects at the border of the domains which in turn favors CLPs insertion and membrane disturbance. It has indeed been reported that in presence of phase coexistence, SRF inserts preferentially at the boundary between phases [66] and presents a higher binding affinity for lipid vesicles presenting a phase coexistence [33]. The initial rate of SRF-induced membrane leakage was also higher in DPPC:POPC vesicles [82], which exhibit phase separation [83], compared to POPC vesicles. The importance of phase coexistence has been less studied for FGC but preferential insertion at phases boundary has also been suggested [52]. The lipid phase separation has already been reported as a key parameter for the ability of nystatin, an antifungal drug, to form pore into membrane [84]. In fungal membranes, sphingolipids are important players in domain segregation [38]. Therefore, the inhibition of nystatin activity in *Saccharomyces cerevisiae* mutant with altered sphingolipid composition supports the importance of phase separation for biological activities of nystatin [38,85], and more broadly membrane-active molecules.

Besides the role of sphingolipids and sterols, a lower CLPs-induced leakage was observed in the fungal model compared to the plant model. The differences between these models lie in the presence of the negatively charged lipid POPG in the fungal model and in the difference in the number of unsaturations in the lipid chains, i.e. one unsaturation in the fungal model and two unsaturations in the plant model. The influence of PG presence in the membrane on both SRF and FGC activity has previously been studied and showed to have a negative impact on the FGC-induced leakage and a positive impact on the SRF-induced leakage [29]. This is consistent with the lower FGC-induced leakage we observed in the fungal model compared to the plant model but it contrasts with our slightly lower SRF-induced leakage observed in the fungal model compared to the plant model. A possible explanation for SRF could arise from differences in the number of acyl chain unsaturations that impacts the affinity of SRF for lipid membranes, with a higher affinity for PLPC compared to POPC [33]. Thus, both negatively charged

lipids and acyl chain unsaturation may play a role in the activity of CLPs. It nevertheless remains difficult to clearly establish individual contribution of the two components based on our present data.

5. Conclusion

Distinct biocontrol activities of SRF and FGC, whether by stimulating plant immunity or by direct antagonism against plant pathogens, strongly correlates with their specific interaction processes with lipid membranes. CLPs are primarily known for their ability to destabilize membrane, notably through pore formation [14]. Our observations indicate that changes in the membrane physical state also contribute to biological properties of CLPs.

To fully grasp the significance of these membrane-related activities in reducing plant infection by SRF and FGC, further complementary experiments are needed. Other lipopeptides might exert a similar effect, and investigating their capacity to alter membrane physical state could offer additional insights into their potential biological effects. In addition, gaining a deeper understanding of the interplay between membrane activity and biological activity of membrane-active molecules could provide valuable information to the rational design and implementation of CLPs as biocontrol agents.

It is worth noting that this study specifically focused on activities related to plant biocontrol. However, disturbance of membrane lipid organization and structure could unveil other interesting properties, such as antiviral [86–88], antibacterial [89] or antitumoral activities [90]. Therefore, considering the impact on membrane lipid packing alongside the leakage mechanism is essential for understanding and predicting the biological activities of CLPs.

Funding

G.G. is recipient of a F.R.I.A. fellowship (Belgian Fund for Scientific Research, F.R.S.-FNRS, grant n° 1.E.069.20F), M.D. and M.O. are respectively senior research associate and research director at the F.R.S.-FNRS. The research was supported by the Feder program 2021-2027 (project PHENIX biocontrol Uliege-SPW) and the PDR Project Surfasymm (F.R.S.-FNRS, grant T.0063.19).

CRediT authorship contribution statement

Marc Ongena: Writing – review & editing, Resources. **Caroline De Clerck:** Writing – review & editing, Resources, Methodology, Conceptualization. **Farah Boubsi:** Writing – review & editing, Investigation. **Haissam Jijakli:** Resources. **Guillaume Gilliard:** Writing – review & editing, Writing – original draft, Methodology, Investigation, Formal analysis, Conceptualization. **Thomas Demortier:** Writing – review & editing, Investigation, Formal analysis. **Magali Deleu:** Writing – review & editing, Supervision, Resources, Project administration, Methodology, Funding acquisition, Conceptualization.

Declaration of Competing Interest

The authors declare that they have no known competing financial interests or personal relationships that could have appeared to influence the work reported in this paper.

Data availability

Data will be made available on request.

Acknowledgments

We thank Ayoub Kaoun for its technical support, Aurelien Furlan and Willy Smeralda for fruitful discussions and Pr Aurore Richel for giving us access to the DLS instrument.

Appendix A. Supporting information

Supplementary data associated with this article can be found in the online version at doi:10.1016/j.colsurfb.2024.113933.

References

[1] F.P. Carvalho, Pesticides, environment, and food safety, Food Energy Secur. 6 (2017) 48–60, https://doi.org/10.1002/fes3.108.
[2] A. Sharma, V. Kumar, B. Shahzad, M. Tanveer, G.P.S. Sidhu, N. Handa, S.K. Kohli, P. Yadav, A.S. Bali, R.D. Parihar, O.I. Dar, K. Singh, S. Jasrotia, P. Bakshi, M. Ramakrishnan, S. Kumar, R. Bhardwaj, A.K. Thukral, Worldwide pesticide usage and its impacts on ecosystem, SN Appl. Sci. 1 (2019) 1446, https://doi.org/10.1007/s42452-019-1485-1.
[3] S.L. Rumschlag, M.B. Mahon, J.T. Hoverman, T.R. Raffel, H.J. Carrick, P.J. Hudson, J.R. Rohr, Consistent effects of pesticides on community structure and ecosystem function in freshwater systems, Nat. Commun. 11 (2020) 6333, https://doi.org/10.1038/s41467-020-20192-2.
[4] R. Seppelt, S. Klotz, E. Peiter, M. Volk, Agriculture and food security under a changing climate: an underestimated challenge, iScience 25 (2022) 105551, https://doi.org/10.1016/j.isci.2022.105551.
[5] S.F. Syed Ab Rahman, E. Singh, C.M.J. Pieterse, P.M. Schenk, Emerging microbial biocontrol strategies for plant pathogens, Plant Sci. 267 (2018) 102–111, https://doi.org/10.1016/j.plantsci.2017.11.012.
[6] Y. Bektas, T. Eulgem, Synthetic plant defense elicitors, Front. Plant Sci. 5 (2015). ⟨https://www.frontiersin.org/articles/10.3389/fpls.2014.00804⟩ (accessed June 6, 2023).
[7] Z. Khatoon, S. Huang, M. Rafique, A. Fakhar, M.A. Kamran, G. Santoyo, Unlocking the potential of plant growth-promoting rhizobacteria on soil health and the sustainability of agricultural systems, J. Environ. Manag. 273 (2020) 111118, https://doi.org/10.1016/j.jenvman.2020.111118.
[8] W. Desmedt, B. Vanholme, T. Kyndt, Chapter 5 - Plant defense priming in the field: a review, in: P. Maienfisch, S. Mangelinckx (Eds.), Recent Highlights in the Discovery and Optimization of Crop Protection Products, Academic Press, 2021, pp. 87–124, https://doi.org/10.1016/B978-0-12-821035-2.00045-0.
[9] J. Pršić, M. Ongena, Elicitors of plant immunity triggered by beneficial bacteria, Front. Plant Sci. 11 (2020). ⟨https://www.frontiersin.org/articles/10.3389/fpls.2020.594530⟩ (accessed July 6, 2022).
[10] J. Crouzet, A. Arguelles-Arias, S. Dhondt-Cordelier, S. Cordelier, J. Pršić, G. Hoff, F. Mazeyrat-Gourbeyre, F. Baillieul, C. Clément, M. Ongena, S. Dorey, Biosurfactants in plant protection against diseases: rhamnolipids and lipopeptides case study, Front. Bioeng. Biotechnol. 8 (2020). ⟨https://www.frontiersin.org/articles/10.3389/fbioe.2020.01014⟩ (accessed June 14, 2023).
[11] M. Fazle Rabbee, K.-H. Baek, Antimicrobial activities of lipopeptides and polyketides of Bacillus velezensis for agricultural applications, Molecules 25 (2020) 4973, https://doi.org/10.3390/molecules25214973.
[12] K. Steinke, O.S. Mohite, T. Weber, Á.T. Kovács, Phylogenetic distribution of secondary metabolites in the bacillus subtilis species complex, 10.1128/msystems.00057-21, mSystems 6 (2021), https://doi.org/10.1128/msystems.00057-21.
[13] A. Théatre, A.C.R. Hoste, A. Rigolet, I. Benneceur, M. Bechet, M. Ongena, M. Deleu, P. Jacques, Bacillus sp.: a remarkable source of bioactive lipopeptides, in: R. Hausmann, M. Henkel (Eds.), Biosurfactants for the Biobased Economy, Springer International Publishing, Cham, 2022, pp. 123–179, https://doi.org/10.1007/10_2021_182.
[14] D. Balleza, A. Alessandrini, M.J. Beltrán García, Role of lipid composition, physicochemical interactions, and membrane mechanics in the molecular actions of microbial cyclic lipopeptides, J. Membr. Biol. 252 (2019) 131–157, https://doi.org/10.1007/s00232-019-00067-4.
[15] M. Kracht, H. Rokos, M. Özel, M. Kowall, G. Pauli, J. Vater, Antiviral and hemolytic activities of surfactin isoforms and their methyl ester derivatives, J. Antibiot. 52 (1999) 613–619, https://doi.org/10.7164/antibiotics.52.613.
[16] L. Yuan, S. Zhang, Y. Wang, Y. Li, X. Wang, Q. Yang, Surfactin inhibits membrane fusion during invasion of epithelial cells by enveloped viruses, J. Virol. 92 (2018) e00809-18, https://doi.org/10.1128/JVI.00809-18.
[17] H. Cawoy, M. Mariutto, G. Henry, C. Fisher, N. Vasilyeva, P. Thonart, J. Dommes, M. Ongena, Plant defense stimulation by natural isolates of bacillus depends on efficient surfactin production, MPMI 27 (2014) 87–100, https://doi.org/10.1094/MPMI-09-13-0262-R.
[18] V.B. Lam, T. Meyer, A.A. Arias, M. Ongena, F.E. Oni, M. Höfte, Bacillus cyclic lipopeptides iturin and fengycin control rice blast caused by Pyricularia oryzae in potting and acid sulfate soils by direct antagonism and induced systemic resistance, Microorganisms 9 (2021) 1441, https://doi.org/10.3390/microorganisms9071441.
[19] P. Xiao, X. Tian, P. Zhu, Y. Xu, C. Zhou, The use of surfactin in inhibiting Botrytis cinerea and in protecting winter jujube from the gray mold, AMB Express 13 (2023) 37, https://doi.org/10.1186/s13568-023-01543-w.
[20] A. Farzand, A. Moosa, M. Zubair, A.R. Khan, V.C. Massawe, H.A.S. Tahir, T.M. M. Sheikh, M. Ayaz, X. Gao, Suppression of sclerotinia sclerotiorum by the induction of systemic resistance and regulation of antioxidant pathways in tomato using fengycin produced by Bacillus amyloliquefaciens FZB42, Biomolecules 9 (2019) 613, https://doi.org/10.3390/biom9100613.
[21] H. Desmyttere, C. Deweer, J. Muchembled, K. Sahmer, J. Jacquin, F. Coutte, P. Jacques, Antifungal activities of bacillus subtilis lipopeptides to two Venturia

inaequalis strains possessing different tebuconazole sensitivity, Front. Microbiol. 10 (2019). ⟨https://www.frontiersin.org/articles/10.3389/fmicb.2019.02327⟩ (accessed October 3, 2022).
[22] Y. Tao, X. Bie, F. Lv, H. Zhao, Z. Lu, Antifungal activity and mechanism of fengycin in the presence and absence of commercial surfactin against Rhizopus stolonifer, J. Microbiol 49 (2011) 146–150, https://doi.org/10.1007/s12275-011-0171-9.
[23] C. Wise, J. Falardeau, I. Hagberg, T.J. Avis, Cellular lipid composition affects sensitivity of plant pathogens to fengycin, an antifungal compound produced by Bacillus subtilis strain CU12, Phytopathology 104 (2014) 1036–1041, https://doi.org/10.1094/PHYTO-12-13-0336-R.
[24] G. Le Mire, A. Siah, M.-N. Brisset, M. Gaucher, M. Deleu, M.H. Jijakli, Surfactin protects wheat against Zymoseptoria tritici and activates both salicylic acid- and jasmonic acid-dependent defense responses, Agriculture 8 (2018) 11, https://doi.org/10.3390/agriculture8010011.
[25] L. Lilge, N. Ersig, P. Hubel, M. Aschern, E. Pillai, P. Klausmann, J. Pfannstiel, M. Henkel, K. Morabbi Heravi, R. Hausmann, Surfactin shows relatively low antimicrobial activity against Bacillus subtilis and other bacterial model organisms in the absence of synergistic metabolites, Microorganisms 10 (2022) 779, https://doi.org/10.3390/microorganisms10040779.
[26] M. Ongena, E. Jourdan, A. Adam, M. Paquot, A. Brans, B. Joris, J.-L. Arpigny, P. Thonart, Surfactin and fengycin lipopeptides of Bacillus subtilis as elicitors of induced systemic resistance in plants, Environ. Microbiol. 9 (2007) 1084–1090, https://doi.org/10.1111/j.1462-2920.2006.01202.x.
[27] G. Wu, Y. Liu, Y. Xu, G. Zhang, Q. Shen, R. Zhang, Exploring elicitors of the beneficial Rhizobacterium Bacillus amyloliquefaciens SQR9 to induce plant systemic resistance and their interactions with plant signaling pathways, MPMI 31 (2018) 560–567, https://doi.org/10.1094/MPMI-11-17-0273-R.
[28] G. Gilliard, A.L. Furlan, W. Smeralda, J. Pršić, M. Deleu, Added value of biophysics to study lipid-driven biological processes: the case of surfactins, a class of natural amphiphile molecules, Int. J. Mol. Sci. 23 (2022) 13831, https://doi.org/10.3390/ijms232213831.
[29] S. Fiedler, H. Heerklotz, Vesicle leakage reflects the target selectivity of antimicrobial lipopeptides from Bacillus subtilis, Biophys. J. 109 (2015) 2079–2089, https://doi.org/10.1016/j.bpj.2015.09.021.
[30] D. Pinkas, R. Fišer, P. Kozlík, T. Dolejšová, K. Hryzáková, I. Konopásek, G. Mikušová, Bacillus subtilis cardiolipin protects its own membrane against surfactin-induced permeabilization, Biochim. Et. Biophys. Acta (BBA) Biomembr. 1862 (2020) 183405, https://doi.org/10.1016/j.bbamem.2020.183405.
[31] P. Uttlová, D. Pinkas, O. Bechyňková, R. Fišer, J. Svobodová, G. Seydlová, Bacillus subtilis alters the proportion of major membrane phospholipids in response to surfactin exposure, Biochim. Et. Biophys. Acta (BBA) Biomembr. 1858 (2016) 2965–2971, https://doi.org/10.1016/j.bbamem.2016.09.006.
[32] H. Patel, C. Tscheka, K. Edwards, G. Karlsson, H. Heerklotz, All-or-none membrane permeabilization by fengycin-type lipopeptides from Bacillus subtilis QST713, Biochim. Et. Biophys. Acta (BBA) Biomembr. 1808 (2011) 2000–2008, https://doi.org/10.1016/j.bbamem.2011.04.008.
[33] G. Henry, M. Deleu, E. Jourdan, P. Thonart, M. Ongena, The bacterial lipopeptide surfactin targets the lipid fraction of the plant plasma membrane to trigger immune-related defence responses, Cell. Microbiol. 13 (2011) 1824–1837, https://doi.org/10.1111/j.1462-5822.2011.01664.x.
[34] M. Deleu, J.-M. Crowet, M.N. Nasir, L. Lins, Complementary biophysical tools to investigate lipid specificity in the interaction between bioactive molecules and the plasma membrane: a review, Biochim. Et. Biophys. Acta (BBA) Biomembr. 1838 (2014) 3171–3190, https://doi.org/10.1016/j.bbamem.2014.08.023.
[35] A. Mamode Cassim, P. Gouguet, J. Gronnier, N. Laurent, V. Germain, M. Grison, Y. Boutté, P. Gerbeau-Pissot, F. Simon-Plas, S. Mongrand, Plant lipids: key players of plasma membrane organization and function, Prog. Lipid Res 73 (2019) 1–27, https://doi.org/10.1016/j.plipres.2018.11.002.
[36] D.G. Sant, S.G. Tupe, C.V. Ramana, M.V. Deshpande, Fungal cell membrane—promising drug target for antifungal therapy, J. Appl. Microbiol. 121 (2016) 1498–1510, https://doi.org/10.1111/jam.13301.
[37] M. Doktorova, J.L. Symons, I. Levental, Structural and functional consequences of reversible lipid asymmetry in living membranes, Nat. Chem. Biol. 16 (2020) 1321–1330, https://doi.org/10.1038/s41589-020-00688-0.
[38] F.C. Santos, J.T. Marquês, A. Bento-Oliveira, R.F.M. de Almeida, Sphingolipid-enriched domains in fungi, FEBS Lett. 594 (2020) 3698–3718, https://doi.org/10.1002/1873-3468.13986.
[39] E. Sezgin, I. Levental, S. Mayor, C. Eggeling, The mystery of membrane organization: composition, regulation and roles of lipid rafts, Nat. Rev. Mol. Cell Biol. 18 (2017) 361–374, https://doi.org/10.1038/nrm.2017.16.
[40] S. Cordelier, J. Crouzet, G. Gilliard, S. Dorey, M. Deleu, S. Dhondt-Cordelier, Deciphering the role of plant plasma membrane lipids in response to invasion patterns: how could biology and biophysics help, J. Exp. Bot. 73 (2022) 2765–2784, https://doi.org/10.1093/jxb/erab517.
[41] S.G. Hovakeemian, R. Liu, S.H. Gellman, H. Heerklotz, Correlating antimicrobial activity and model membrane leakage induced by nylon-3 polymers and detergents, Soft Matter 11 (2015) 6840–6851, https://doi.org/10.1039/C5SM01521A.
[42] H. Razafindralambo, S. Dufour, M. Paquot, M. Deleu, Thermodynamic studies of the binding interactions of surfactin analogues to lipid vesicles: application of isothermal titration calorimetry, J. Therm. Anal. Calorim. 95 (2009) 817–821, https://doi.org/10.1007/s10973-008-9403-6.
[43] H. Razafindralambo, M. Paquot, C. Hbid, P. Jacques, J. Destain, P. Thonart, Purification of antifungal lipopeptides by reversed-phase high-performance liquid chromatography, J. Chromatogr. A 639 (1993) 81–85, https://doi.org/10.1016/0021-9673(93)83091-6.
[44] M. Deleu, M. Paquot, T. Nylander, Effect of fengycin, a lipopeptide produced by Bacillus subtilis, on model biomembranes, Biophys. J. 94 (2008) 2667–2679, https://doi.org/10.1529/biophysj.107.114090.
[45] G. De Meyer, J. Bigirimana, Y. Elad, M. Höfte, Induced systemic resistance in Trichoderma harzianum T39 biocontrol of Botrytis cinerea, Eur. J. Plant Pathol. 104 (1998) 279–286, https://doi.org/10.1023/A:1008628806616.
[46] J. Maintz, M. Cavdar, J. Tamborski, M. Kwaaitaal, R. Huisman, C. Meesters, E. Kombrink, R. Panstruga, Comparative analysis of MAMP-induced calcium influx in arabidopsis seedlings and protoplasts, Plant Cell Physiol. 55 (2014) 1813–1825, https://doi.org/10.1093/pcp/pcu112.
[47] N. Monnier, A.L. Furlan, S. Buchoux, M. Deleu, M. Dauchez, S. Rippa, C. Sarazin, Exploring the dual interaction of natural rhamnolipids with plant and fungal biomimetic plasma membranes through biophysical studies, Int. J. Mol. Sci. 20 (2019) 1009, https://doi.org/10.3390/ijms20051009.
[48] F. Furt, F. Simon-Plas, S. Mongrand, Lipids of the plant plasma membrane, in: A. S. Murphy, B. Schulz, W. Peer (Eds.), The Plant Plasma Membrane, Springer Berlin Heidelberg, Berlin, Heidelberg, 2011, pp. 3–30, https://doi.org/10.1007/978-3-642-13431-9_1.
[49] J.-L. Cacas, C. Buré, K. Grosjean, P. Gerbeau-Pissot, J. Lherminier, Y. Rombouts, E. Maes, C. Bossard, J. Gronnier, F. Furt, L. Fouillen, V. Germain, E. Bayer, S. Cluzet, F. Robert, J.-M. Schmitter, M. Deleu, L. Lins, F. Simon-Plas, S. Mongrand, Revisiting plant plasma membrane lipids in tobacco: a focus on sphingolipids, Plant Physiol. 170 (2016) 367–384, https://doi.org/10.1104/pp.15.00564.
[50] G. Hoff, A. Arguelles Arias, F. Boubsi, J. Pršić, T. Meyer, H.M.M. Ibrahim, S. Steels, P. Luzuriaga, A. Legras, L. Franzil, M. Lequart-Pillon, C. Rayon, V. Osorio, E. de Pauw, Y. Lara, E. Deboever, B. de Coninck, P. Jacques, M. Deleu, E. Petit, O. Van Wuytswinkel, M. Ongena, Surfactin stimulated by pectin molecular patterns and root exudates acts as a key driver of the bacillus-plant mutualistic interaction, e01774-21, mBio 12 (2021), https://doi.org/10.1128/mBio.01774-21.
[51] R. Dean, J. a L. Van Kan, Z.A. Pretorius, K.E. Hammond-Kosack, A. Di Pietro, P. D. Spanu, J.J. Rudd, M. Dickman, R. Kahmann, J. Ellis, G.D. Foster, The top 10 fungal pathogens in molecular plant pathology, Mol. Plant Pathol. 13 (2012) 414–430, https://doi.org/10.1111/j.1364-3703.2011.00783.x.
[52] M. Eeman, G. Olofsson, E. Sparr, M.N. Nasir, T. Nylander, M. Deleu, Interaction of fengycin with stratum corneum mimicking model membranes: a calorimetry study, Colloids Surf. B: Biointerfaces 121 (2014) 27–35, https://doi.org/10.1016/j.colsurfb.2014.05.019.
[53] B.P.M. Ngou, P. Ding, J.D.G. Jones, Thirty years of resistance: Zig-zag through the plant immune system, Plant Cell 34 (2022) 1447–1478, https://doi.org/10.1093/plcell/koac041.
[54] E. Jourdan, G. Henry, F. Duby, J. Dommes, J.P. Barthélemy, P. Thonart, M. Ongena, Insights into the defense-related events occurring in plant cells following perception of surfactin-type lipopeptide from Bacillus subtilis, MPMI 22 (2009) 456–468, https://doi.org/10.1094/MPMI-22-4-0456.
[55] A.S. Klymchenko, Solvatochromic and fluorogenic dyes as environment-sensitive probes: design and biological applications, Acc. Chem. Res. 50 (2017) 366–375, https://doi.org/10.1021/acs.accounts.6b00517.
[56] A. Makovitzki, D. Avrahami, Y. Shai, Ultrashort antibacterial and antifungal lipopeptides, Proc. Natl. Acad. Sci. 103 (2006) 15997–16002, https://doi.org/10.1073/pnas.0606129103.
[57] H.Y. Fan, M. Nazari, G. Raval, Z. Khan, H. Patel, H. Heerklotz, Utilizing zeta potential measurements to study the effective charge, membrane partitioning, and membrane permeation of the lipopeptide surfactin, Biochim. Et. Biophys. Acta (BBA) - Biomembr. 1838 (2014) 2306–2312, https://doi.org/10.1016/j.bbamem.2014.02.018.
[58] S.J. Wallace, J. Li, R.L. Nation, B.J. Boyd, Drug release from nanomedicines: selection of appropriate encapsulation and release methodology, Drug Deliv. Transl. Res. 2 (2012) 284–292, https://doi.org/10.1007/s13346-012-0064-4.
[59] C.H. Crouch, M.H. Bost, T.H. Kim, B.M. Green, D.S. Arbuckle, C.H. Grossman, K. P. Howard, Optimization of detergent-mediated reconstitution of influenza A M2 protein into proteoliposomes, Membranes 8 (2018) 103, https://doi.org/10.3390/membranes8040103.
[60] C. Botcazon, T. Bergia, D. Lecouturier, C. Dupuis, A. Rochex, S. Acket, P. Nicot, V. Leclère, C. Sarazin, S. Rippa, Rhamnolipids and fengycins, very promising amphiphilic antifungal compounds from bacteria secretomes, act on Sclerotiniaceae fungi through different mechanisms, Front. Microbiol. 13 (2022). ⟨https://www.frontiersin.org/articles/10.3389/fmicb.2022.977633⟩ (accessed August 25, 2023).
[61] H. Patel, Q. Huynh, D. Bärlehner, H. Heerklotz, Additive and Synergistic Membrane Permeabilization by Antimicrobial (Lipo)Peptides and Detergents, Biophys. J. 106 (2014) 2115–2125, https://doi.org/10.1016/j.bpj.2014.04.006.
[62] H. Heerklotz, J. Seelig, Leakage and lysis of lipid membranes induced by the lipopeptide surfactin, Eur. Biophys. J. 36 (2007) 305–314, https://doi.org/10.1007/s00249-006-0091-5.
[63] A. Hossein, M. Deserno, Spontaneous curvature, differential stress, and bending modulus of asymmetric lipid membranes, Biophys. J. 118 (2020) 624–642, https://doi.org/10.1016/j.bpj.2019.11.3398.
[64] H. Heerklotz, Interactions of surfactants with lipid membranes, Q. Rev. Biophys. 41 (2008) 205–264, https://doi.org/10.1017/S0033583508004721.
[65] M. Doktorova, J.L. Symons, X. Zhang, H.-Y. Wang, J. Schlegel, J.H. Lorent, F.A. Heberle, E. Sezgin, E. Lyman, K.R. Levental, I. Levental, 2023, , Levental, Cell Membranes Sustain Phospholipid Imbalance Via Cholesterol Asymmetry10.1101/2023.07.30.551157 2023.07.30.551157.
[66] M. Deleu, J. Lorent, L. Lins, R. Brasseur, N. Braun, K. El Kirat, T. Nylander, Y. F. Dufrêne, M.-P. Mingeot-Leclercq, Effects of surfactin on membrane models

displaying lipid phase separation, Biochim. Et. Biophys. Acta (BBA) Biomembr. 1828 (2013) 801–815, https://doi.org/10.1016/j.bbamem.2012.11.007.
[67] L.M. González-Jaramillo, F.J. Aranda, J.A. Teruel, V. Villegas-Escobar, A. Ortiz, Antimycotic activity of fengycin C biosurfactant and its interaction with phosphatidylcholine model membranes, Colloids Surf. B: Biointerfaces 156 (2017) 114–122, https://doi.org/10.1016/j.colsurfb.2017.05.021.
[68] E. Mantil, T. Crippin, T.J. Avis, Domain redistribution within ergosterol-containing model membranes in the presence of the antimicrobial compound fengycin, Biochim. Et. Biophys. Acta (BBA) Biomembr. 1861 (2019) 738–747, https://doi.org/10.1016/j.bbamem.2019.01.003.
[69] H. Cawoy, D. Debois, L. Franzil, E. De Pauw, P. Thonart, M. Ongena, Lipopeptides as main ingredients for inhibition of fungal phytopathogens by Bacillus subtilis/amyloliquefaciens, Microb. Biotechnol. 8 (2015) 281–295, https://doi.org/10.1111/1751-7915.12238.
[70] F. Ackermann, T. Stanislas, The plasma membrane—an integrating compartment for mechano-signaling, Plants 9 (2020) 505, https://doi.org/10.3390/plants9040505.
[71] J.M. Codjoe, K. Miller, E.S. Haswell, Plant cell mechanobiology: greater than the sum of its parts, Plant Cell 34 (2022) 129–145, https://doi.org/10.1093/plcell/koab230.
[72] T. Ukawa, F. Banno, T. Ishikawa, K. Kasahara, Y. Nishina, R. Inoue, K. Tsujii, M. Yamaguchi, T. Takahashi, Y. Fukao, M. Kawai-Yamada, M. Nagano, Sphingolipids with 2-hydroxy fatty acids aid in plasma membrane nanodomain organization and oxidative burst, Plant Physiol. 189 (2022) 839–857, https://doi.org/10.1093/plphys/kiac134.
[73] B. Martinac, J. Adler, C. Kung, Mechanosensitive ion channels of E. coli activated by amphipaths, Nature 348 (1990) 261–263, https://doi.org/10.1038/348261a0.
[74] A.J. Patel, E. Honoré, F. Maingret, F. Lesage, M. Fink, F. Duprat, M. Lazdunski, A mammalian two pore domain mechano-gated S-like K+ channel, EMBO J. 17 (1998) 4283–4290, https://doi.org/10.1093/emboj/17.15.4283.
[75] R. Almeida, E. Joly, Crystallization around solid-like nanosized docks can explain the specificity, diversity, and stability of membrane microdomains, Front. Plant Sci. 5 (2014). ⟨https://www.frontiersin.org/articles/10.3389/fpls.2014.00072⟩ (accessed September 6, 2023).
[76] G. Francius, S. Dufour, M. Deleu, M. Paquot, M.-P. Mingeot-Leclercq, Y.F. Dufrêne, Nanoscale membrane activity of surfactins: influence of geometry, charge and hydrophobicity, Biochim. Et. Biophys. Acta (BBA) - Biomembr. 1778 (2008) 2058–2068, https://doi.org/10.1016/j.bbamem.2008.03.023.
[77] N. Geudens, M.N. Nasir, J.-M. Crowet, J.M. Raaijmakers, K. Fehér, T. Coenye, J. C. Martins, L. Lins, D. Sinnaeve, M. Deleu, Membrane Interactions of Natural Cyclic Lipodepsipeptides of the Viscosin Group, Biochim. Et. Biophys. Acta (BBA) - Biomembr. 1859 (2017) 331–339, https://doi.org/10.1016/j.bbamem.2016.12.013.
[78] E. Mantil, I. Buznytska, G. Daly, A. Ianoul, T.J. Avis, Role of lipid composition in the interaction and activity of the antimicrobial compound fengycin with complex membrane models, J. Membr. Biol. 252 (2019) 627–638, https://doi.org/10.1007/s00232-019-00100-6.
[79] V. Rondelli, A. Koutsioubas, J. Pršić, E. Deboever, J.M. Crowet, L. Lins, M. Deleu, Sitosterol and glucosylceramide cooperative transversal and lateral uneven distribution in plant membranes, Sci. Rep. 11 (2021) 21618, https://doi.org/10.1038/s41598-021-00696-7.
[80] R.F.M. de Almeida, A. Fedorov, M. Prieto, Sphingomyelin/phosphatidylcholine/cholesterol phase diagram: boundaries and composition of lipid rafts, Biophys. J. 85 (2003) 2406–2416, https://doi.org/10.1016/S0006-3495(03)74664-5.
[81] J.C. Lawrence, D.E. Saslowsky, J. Michael Edwardson, R.M. Henderson, Real-time analysis of the effects of cholesterol on lipid raft behavior using atomic force microscopy, Biophys. J. 84 (2003) 1827–1832, https://doi.org/10.1016/S0006-3495(03)74990-X.
[82] C. Carrillo, J.A. Teruel, F.J. Aranda, A. Ortiz, Molecular mechanism of membrane permeabilization by the peptide antibiotic surfactin, Biochim. Et. Biophys. Acta (BBA) - Biomembr. 1611 (2003) 91–97, https://doi.org/10.1016/S0005-2736(03)00029-4.
[83] C.J. Garvey, S.J. Bryant, A. Elbourne, T. Hunt, B. Kent, M. Kreuzer, M. Strobl, R. Steitz, G. Bryant, Phase separation in a ternary DPPC/DOPC/POPC system with reducing hydration, J. Colloid Interface Sci. 638 (2023) 719–732, https://doi.org/10.1016/j.jcis.2023.01.145.
[84] A.G. dos Santos, J.T. Marquês, A.C. Carreira, I.R. Castro, A.S. Viana, M.-P. Mingeot-Leclercq, R.F.M. de Almeida, L.C. Silva, The molecular mechanism of Nystatin action is dependent on the membrane biophysical properties and lipid composition, Phys. Chem. Chem. Phys. 19 (2017) 30078–30088, https://doi.org/10.1039/C7CP05353C.
[85] A. Leber, P. Fischer, R. Schneiter, S.D. Kohlwein, G. Daum, The yeast mic2 mutant is defective in the formation of mannosyl-diinositolphosphorylceramide1This study was supported by the Fonds zur Förderung der wissenschaftlichen Forschung in Österreich (project S-5811 to G.D., and project 11731 to S.D.K.).1, FEBS Lett. 411 (1997) 211–214, https://doi.org/10.1016/S0014-5793(97)00692-3.
[86] K. Matsuda, S. Hattori, R. Kariya, Y. Komizu, E. Kudo, H. Goto, M. Taura, R. Ueoka, S. Kimura, S. Okada, Inhibition of HIV-1 entry by the tricyclic coumarin GUT-70 through the modification of membrane fluidity, Biochem. Biophys. Res. Commun. 457 (2015) 288–294, https://doi.org/10.1016/j.bbrc.2014.12.102.
[87] S. Harada, The broad anti-viral agent glycyrrhizin directly modulates the fluidity of plasma membrane and HIV-1 envelope, Biochem J. 392 (2005) 191–199, https://doi.org/10.1042/BJ20051069.
[88] C.C. Anggakusuma, L.M. Colpitts, H. Schang, A. Rachmawati, S. Frentzen, P. Pfaender, R.J.P. Behrendt, D. Brown, J. Bankwitz, M. Steinmann, P. Ott, C. M. Meuleman, A. Rice, T. Ploss, E. Pietschmann, Steinmann, Turmeric curcumin inhibits entry of all hepatitis C virus genotypes into human liver cells, Gut 63 (2014) 1137–1149, https://doi.org/10.1136/gutjnl-2012-304299.
[89] S. Omardien, J.W. Drijfhout, F.M. Vaz, M. Wenzel, L.W. Hamoen, S.A.J. Zaat, S. Brul, Bactericidal activity of amphipathic cationic antimicrobial peptides involves altering the membrane fluidity when interacting with the phospholipid bilayer, Biochim. Et. Biophys. Acta (BBA) Biomembr. 1860 (2018) 2404–2415, https://doi.org/10.1016/j.bbamem.2018.06.004.
[90] S. Selvaraj, S. Krishnaswamy, V. Devashya, S. Sethuraman, U.M. Krishnan, Influence of membrane lipid composition on flavonoid–membrane interactions: implications on their biological activity, Prog. Lipid Res. 58 (2015) 1–13, https://doi.org/10.1016/j.plipres.2014.11.002.